

Radiologically Undetected Hepatocellular Carcinoma in Patients Undergoing Liver Transplantation

An Immunohistochemical Correlation With LI-RADS Score

Wei Xiong, MD, PhD,* Gregory Cheeney, MD,* Sooah Kim, MD,† Violetta Kolesnikova, MD, PhD,* Brooke Henninger, MD,* Jacob Alexander, MD,‡ Paul E. Swanson, MD,* Melissa P. Upton, MD,* Camtu D. Truong, MD,* and Matthew M. Yeh, MD, PhD*‡

Abstract: Orthotopic liver transplantation is the best option for patients with carefully selected unresectable disease because of underlying liver dysfunction. The 5-year survival rate after orthotopic liver transplantation for early detected hepatocellular carcinoma (HCC) is high, and a similar or even higher rate is reported in those with radiologically undetected HCC. This study evaluated and compared the histologic features of pretransplant radiologically undetected (14 patients, 25 tumors) versus detected (36 patients, 45 tumors) HCCs. Tumor size, tumor differentiation, number of unpaired arteries, mitotic count per 10 high-power fields, CD34 immunostain to assess microvessel density, and Ki67 immunostain were compared with the Liver Imaging Reporting and Data System score, which was retrospectively assigned to each tumor in both groups. The Liver Imaging Reporting and Data System score was significantly higher in the HCC detected group ($P < 0.001$). The vast majority of the undetected HCCs (88%) was < 2 cm in size. Only 12% of the undetected HCCs were ≥ 2 cm, whereas 51% of the detected HCCs were ≥ 2 cm in size. Higher rate of moderate to poor tumor differentiation was noted in the detected HCCs compared with the undetected group (89% vs. 60%; $P = 0.004$). No statistically significant difference in the number and distribution of unpaired arteries, or mitotic count was observed in 2 groups (although fewer unpaired arteries were identified in the undetected group). The detected HCCs had a higher rate of 2+ CD34 staining compared with the undetected HCCs (68% vs. 27%; $P = 0.002$), whereas the opposite was observed for 1+ CD34 staining (59% undetected HCCs vs. 17% detected HCCs; $P = 0.002$). Ki67 proliferative index was not statistically different between the 2 groups (120.8/1000 cells detected HCCs vs. 81.8/1000 cells undetected HCCs; $P = 0.36$). The factors associated

with failing to detect HCCs pretransplant by radiologic studies include small tumor size (< 2 cm), low-grade histologic differentiation, and low microvessel density (low CD34 staining). A significant association between the number and distribution of unpaired arteries and HCC detection has not been established by our study.

Key Words: hepatocellular carcinoma, transplant, liver, undetected, LI-RADS, score, immunohistochemistry, CD34, Ki67 (*Am J Surg Pathol* 2017;41:1466–1472)

BACKGROUND

Hepatocellular carcinoma (HCC) is the one of the most common malignancies worldwide, and its incidence is rising in the United States.^{1–3} Patients with cirrhosis, including those with hepatitis B and C virus infection, and alcohol and nonalcoholic fatty liver diseases are at risk of developing HCC. The overall prognosis for HCC is poor, especially if it is not detected at an early stage. Patients at high risk for HCC are recommended to undergo screening and surveillance to detect hepatocellular neoplasms at earlier stage.⁴ Orthotopic liver transplantation (OLT) has been proven to offer the best chance for cure in those with carefully selected unresectable disease because of underlying liver dysfunction.⁵ Recent studies show that OLT for early-stage HCC has a 5-year survival rate of 75% to 83%.⁵ A similar or even more favorable outcome was reported in patients with undetected or unexpected HCC at the time of liver transplantation.^{6–8}

According to American Association for the Study of Liver Diseases, surveillance for HCC includes alpha-fetoprotein and ultrasonography.^{4,9} In patients with nodules 1 to 2 cm on ultrasound screening, dynamic imaging studies, either computed tomography (CT) or magnetic resonance with contrast, contrast ultrasound, or biopsy, if needed, are recommended.^{4,9,10} The neoangiogenesis of HCC is commonly characterized by a deterioration of arterial blood flow and the loss of portal blood flow.¹¹ Consequently, the portal blood flow decreases with the advancement of tumor, and the tumor is eventually fed predominantly by the arterial flow. The change in the

From the Departments of *Pathology; †Radiology; and ‡Medicine, University of Washington School of Medicine, Seattle, WA. W.X. and G.C. contributed equally.

Conflicts of Interest and Source of Funding: The authors have disclosed that they have no significant relationships with, or financial interest in, any commercial companies pertaining to this article.

Correspondence: Matthew M. Yeh, MD, PhD, Department of Pathology, University of Washington School of Medicine, 1959 NE Pacific Street, NE140D, P.O. Box 356100, Seattle, WA 98195 (e-mail: myeh@u.washington.edu).

Copyright © 2017 Wolters Kluwer Health, Inc. All rights reserved.

vascular supply is the biological basis for the imaging diagnosis of HCC within cirrhotic liver.^{12–14} The typical radiologic features of HCC on 3-phase or 4-phase CT (multiphase CT, thereafter) include hyperenhancing masses on a background of a minimally enhanced liver parenchyma during the hepatic arterial phase and washout within the tumor on portal venous and delayed phases.^{10,15}

The CT and magnetic resonance imaging characteristics of suspicious liver lesions in cirrhotic patients have recently been standardized using the Liver Imaging Reporting and Data System (LI-RADS), which has 8 categories.¹⁶ The size and arterial enhancement pattern are the main criteria, with washout, capsule, and threshold growth affecting the final LI-RADS score (Table 1). The sensitivity and specificity of multiphase CT are not optimal, especially for lesions <2 cm.¹⁷ Approximately 30% of HCCs are not detected by radiologic studies in patients with cirrhosis.^{6,18,19}

Very limited studies have systemically evaluated the pathologic features of undetected HCCs by CT-imaging modalities in the OLT patients.^{6,7} For example, 1 study examined only the size, stage, and lymphovascular invasion in 9 undetected HCCs in liver explants.⁶ Understanding the pathologic and biological features of the undetected HCCs may assist in the development of more sensitive and specific radiologic modalities for early HCC detection. In this study, we systemically evaluated the histologic features of the HCCs undetected by standard multiphase CT studies in cirrhotic liver explants compared with the CT-detected HCCs, and compared retrospectively assigned LI-RADS values in 2 groups, as this scheme is currently the most standardized imaging reporting system used and conversed among multidisciplinary health professionals. Given the importance of neoangiogenesis in HCCs, we also examined microvessel density and distribution by CD34 immunohistochemistry. The proliferation rate within HCCs was also evaluated by immunoreactivity for Ki67.

TABLE 1. LI-RADS, Version 2014, Category and Criteria of LR-3, 4, 5

LR-1	Definitely benign				
LR-2	Probably benign				
LR-3	Intermediate probability for HCC				
LR-4	Probably HCC				
LR-5	Definitely HCC				
LR-5V	Definitely HCC with tumor in vein				
LR-M	Probably malignant, not specific for HCC				
LR-treated	Treated observation				
	Arterial phase hypoenhancement or isoenhancement		Arterial phase hyperenhancement		
Diameter (mm)	< 20	≥ 20	< 10	10–19	≥ 20
Washout capsule threshold growth					
None	LR-3	LR-3	LR-3	LR-3	LR-4
1	LR-3	LR-4	LR-4	LR-4/LR-5	LR-5
≥ 2	LR-4	LR-4	LR-4	LR-5	LR-5

LR = LI-RADS.

METHODS

Institutional review board approval was obtained for this retrospective study. We identified 50 adult patients with a pathologic diagnosis of HCC and cirrhosis on native livers removed during OLT between 1999 and 2005 at the University of Washington Medical Center (Seattle, WA), a large tertiary organ transplant center. The inclusion criteria included histologic confirmation of HCC and cirrhosis, availability of paraffin blocks of the tumors for immunohistochemical studies, and available radiologic CT reports for the pretransplant liver. HCCs treated with locoregional therapy, such as chemoembolization or ablation were excluded. We only included CT examinations performed using multiphase (3-phase or 4-phase) dynamic contrast-enhanced liver CT protocols in our study cohort. These cases were included only when radiology reports contained the information about the protocol in the technique section of each report. CT images were obtained using multidetector CT scanners (GE Healthcare, Milwaukee, WI). To keep the study less confounding, we excluded cases in which a single patient had pre-OLT detected HCC(s) and other HCC(s) undetected, or vice versa. Hence, a single patient may have either multiple undetected or detected HCCs, but not both. Our final study cohort included 50 patients: 44 men and 6 women. There were 25 undetected HCCs by CT in 14 patients (mean age, 53.4 ± 11.8). The control group included 45 HCCs from 36 patients (mean age, 55.0 ± 16.2) who were detected by CT and confirmed by pathology in the explant livers during the same period of time.

Initially radiology reports were reviewed and the radiologic diagnosis by CT imaging was categorized as: (1) detected HCC: reported as highly suspicious for HCC, worrisome for HCC, consistent with HCC or HCC versus high-grade dysplastic nodule; (2) no HCC detected: reported as regenerative nodule, cirrhotic liver with no suspicious lesions, or as other benign conditions. And then, each reported lesion based on the radiology report was retrospectively reviewed on a picture archiving and communication system to assign a LI-RADS designation by a university radiologist (S.K.) proficient in LI-RADS scoring. As our CT examinations were performed before the introduction of LI-RADS category, all the imaging features that were essential to categorize LI-RADS score were not always necessarily described in the radiology report. Therefore, it was an essential process that the radiologist needed to review the CT images on picture archiving and communication system to be able to fully evaluate the imaging features and to assign LI-RADS category. For undetected HCC, attempts were made by the same radiologist to localize the lesions on CT imaging based pathology reports. If there were visible lesions on CT that best correlated with the location and size with the pathology reports in retrospect, LI-RADS scores were assigned.

Formalin-fixed paraffin-embedded tissues, including both the HCC and adjacent non-neoplastic liver, were sectioned at a thickness of 4 μ m. Hematoxylin-eosin

staining was performed to verify the morphologic diagnosis of HCC. Histologic sections of HCC from resected specimens were examined by 2 pathologists (B.H. and M.M.Y.) with no knowledge of the preoperative CT findings. The diagnosis of HCC was based on the WHO criteria.²⁰

The pathology and histology of HCCs was examined independently. The following features were assessed: tumor size (based on gross examination), mitotic figures per 10 high-power fields (HPFs), number of unpaired arteries per 10 HPF. The distribution of the unpaired arteries within the tumor was assessed as: central, peripheral, or pan-nodular. Unpaired arteries were defined as arteries that were not accompanied by bile ducts. Other histologic features, including tumor necrosis, bile production, and Mallory-Denk bodies within the tumor were evaluated as none, mild, and severe. Vascular invasion was evaluated as positive or negative. Fat within the tumor was semi-quantitatively assessed as: 0 = < 5%, 1 = 5% to 33%, 2 = 34% to 66%, 3 = 67% to 100%.

To assess sinusoidal capillarization, CD34 labeling of sinusoidal endothelial cells was evaluated in 22 of 25 undetected HCCs and 41 of 45 detected HCCs that had available tissue in our archives for performing immunohistochemistry.

Immunohistochemical studies were performed by using the streptavidin-biotin complex method, with an automated staining system. Monoclonal anti-CD34 (clone QBEnd-10, 1:200; Dako) and anti-Ki67 (clone MIB-1, 1:200; Dako) antibodies were used. Deparaffinized sections were treated with 3% hydrogen peroxide in methanol for 10 minutes to inhibit the activity of endogenous peroxidase. The sections were then incubated with primary antibodies for 30 minutes at room temperature. Following the primary antibodies, each section was treated sequentially with biotinylated secondary antibody and streptavidin-biotin-peroxidase complex (Dako). 3,3'-Diaminobenzidine tetrahydrochloride was used as a chromogen, and Mayer's hematoxylin counterstain was applied. Negative controls were run simultaneously. The extent of CD34-positive staining of sinusoidal endothelial cells was assigned as follows: negative = 0; <33% = 1+; 33% to 66% = 2+; >66% = 3+. The sublocation of the CD34 immunoreactivity was also noted (peripheral, central, or pan-nodular pattern). The proliferative index was defined as ratio of Ki67-labeled tumor nuclei per 1000 tumor cells, counted on high power (×400) in "hot spots."

Statistical analysis (χ^2 test, Student *t* test, and Kruskal-Wallis test) was performed when appropriate. *P*-values of <0.05 were considered to indicate a significant difference.

RESULT

Seventy HCCs from 50 patients were included in our study. Twenty-five HCCs from 14 patients were undetected by the pretransplant CT studies, whereas 45 HCCs from 36 patients were identified in imaging studies. The mean age of patients with the undetected HCCs was not significantly different from the control group (53.4 vs.

TABLE 2. Patient Demographics of Age, Sex, and Etiology of Cirrhosis by Undetected and Detected HCCs

	Undetected HCC (N = 14)	Detected HCC (N = 36)	<i>P</i>
Age (mean ± SD)	53.4 ± 11.8	55.0 ± 16.2	0.49
Sex (M:F)	11:3	33:3	0.33
Cause of cirrhosis			
HCV	9	21	0.72
HBV	2	7	
HBV/HCV	1	4	
ETOH	0	2	
Other	2	2	

There is no significant difference in patient parameters between the 2 groups. ETOH indicates ethanol; F, female; HBV, hepatitis B; HCV, hepatitis C; M, male.

55.0 y; *P* = 0.49, Table 2). A male predominance was observed in both groups (*P* = 0.33, Table 2). The most common cause of cirrhosis was hepatitis C, followed by hepatitis B and alcohol (*P* = 0.72, Table 2) in both groups. Two patients in the undetected HCC group and 1 patient in the detected HCC group had cryptogenic cirrhosis. One patient in the detected HCC group had a diagnosis of autoimmune hepatitis.

Of the 25 HCCs not detected by original CT reports, 10 HCCs were retrospectively identifiable, such that LI-RADS scores were assigned. The LI-RADS scores were unexpectedly low, with 14 not localized, 7 LI-RADS 3, and 3 LI-RADS 4 lesions (1 CT was not available for review). Of the 45 HCCs detected, LI-RADS score was assigned as follows: 2 not localized, 3 LI-RADS 3, 10 LI-RADS 4, and 26 LI-RADS 5. As expected, the LI-RADS score was significantly higher in the HCC detected group (*P* < 0.001).

The vast majority of the undetected HCCs (88%) had a size <2.0 cm. Only 12% of the undetected HCCs were ≥ 2.0 cm, whereas 51% of the detected HCCs were ≥ 2.0 cm (Fig. 1). The sizes of the HCCs were significantly smaller in the undetected group compared with the detected group (1.3 vs. 2.4 cm; *P* = 0.001, Table 3).

A higher number of the detected HCCs exhibited moderate to poor differentiation compared with undetected HCCs (89% vs. 60%; *P* = 0.004, Table 3). Interestingly, the size of the moderately to poorly differentiated HCCs was also significantly different between the undetected and detected groups (1.6 ± 1.0 vs. 2.5 ± 1.3 cm; *P* = 0.03, Fig. 2).

Tumor enhancement in the hepatic arterial phase is an important feature for diagnosis of HCC on CT imaging. We, therefore, evaluated the number and distribution of unpaired arteries on the histologic section of HCCs. There were more unpaired arteries in the moderately to poorly differentiated HCCs than that in the well-differentiated HCCs. The tumors that were missed on radiology had fewer unpaired arteries (10.4 ± 4.9) compared with the detected HCCs (12.8 ± 7.0). However, this difference was not statistically significant (*P* = 0.15, Table 3). In addition, the distribution of the unpaired arteries within the tumor

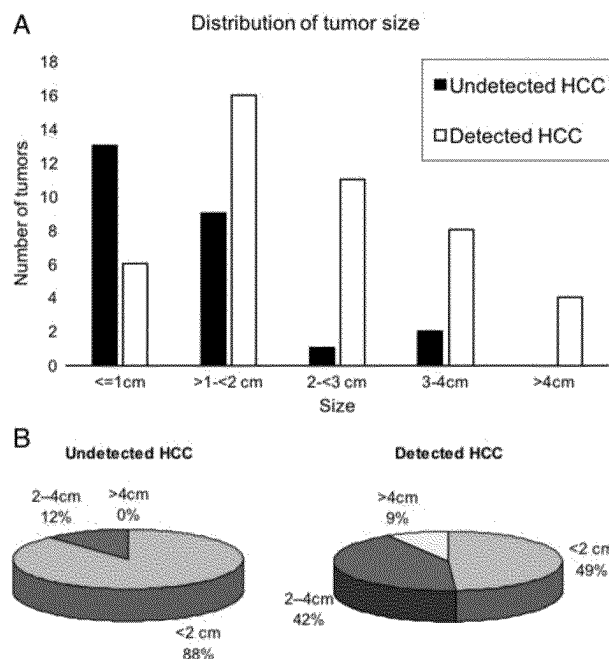


FIGURE 1. A, Distribution of undetected and detected HCC by size of tumor. B, Percentage of undetected and detected lesions <2.0 cm, between 2 and 4 cm, and over 4 cm. The vast majority of undetected HCCs were <2.0 cm.

was not different between the 2 groups ($P=0.0933$). There was no significant difference in the number of unpaired arteries between the detected and the undetected HCCs when

TABLE 3. Tumor Size, Tumor Differentiation, Unpaired Arteries, Mitotic Count, and LI-RADS Score for Undetected and Detected HCCs

	Undetected HCC (25 Tumors)	Detected HCC (45 Tumors)	P
Tumor size (n [%]) (cm)	1.3 (0.6-4.0)	2.4 (0.6-5.0)	0.001
≤ 1	13 (52)	6 (13)	
> 1- < 2	9 (36)	16 (36)	
2- < 3	1 (4)	11 (24)	
3-4	2 (8)	8 (18)	
> 4	0	4 (9)	
Tumor differentiation (n [%])			0.004
Well	10 (40)	5 (11)	
Moderately poorly	15 (60)	40 (89)	
Unpaired arteries (per 10 HPF) (cm)	10.4	12.8	0.15
< 2	11.4	11.5	0.23
2-4	10.3	13.2	0.26
> 4	NA	17.5	NA
Mitotic count (per 10 HPF)	0.3	0.6	0.17
LI-RADS			0.0
Not localized	14	2	
3	7	3	
4	3	10	
5	0	26	

NA indicates not available.

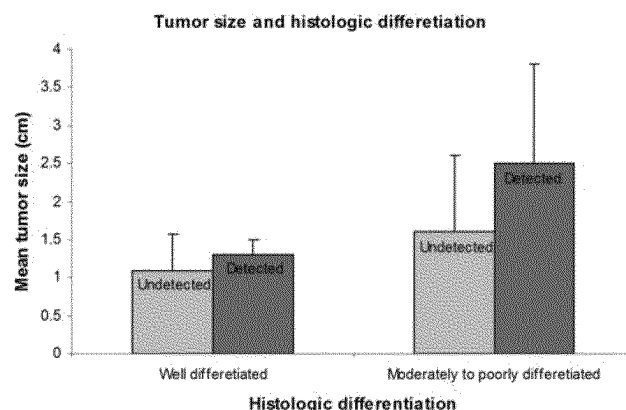


FIGURE 2. The mean tumor size in undetected and detected well differentiated and moderately to poorly differentiated HCC. Detected HCCs exhibited decreased differentiation compared with undetected HCCs. In addition, there was a significant difference between size of the undetected and detected groups within the moderately to poorly differentiated HCCs subgroup.

tumor size and histologic differentiation were controlled for (data not shown).

The mean mitotic count in the undetected HCCs was half that of the detected HCCs (0.3/10 vs. 0.6/10 HPF), but this difference did not reach statistical significance ($P=0.17$, Table 3). We did not observe significant differences in other histologic features between the 2 groups, including tumor necrosis, bile production, Mallory-Denk bodies, fatty change within the tumors, and vascular invasion.

CD34 immunoreactivity to assess sinusoidal capillarization was observed in all the tumors with tissue available for immunohistochemistry. Sixty-eight percent of the detected HCCs demonstrated 2+ CD34 staining (33% to 66% of the sinusoidal space), whereas only 27% of the undetected HCCs showed 2+ CD34 staining. Fifty-nine percent of the undetected HCCs demonstrated 1+ CD34 staining (<33% of the sinusoidal space), whereas only 17% of detected HCCs demonstrated 1+ CD34 staining. The CD34 expression was significantly less diffuse in the undetected HCC group than that in the detected HCC group ($P=0.002$, Table 4 and Fig. 3). The sublocation of the CD34 immunostaining (central vs. peripheral vs. pan-nodular) tended to be different (the undetected HCCs were more likely to have peripheral staining pattern [45%], whereas the detected HCCs were more likely to have pan-nodular distribution [66%]); however, no statistical significance was reached ($P=0.149$, Table 4).

Finally, the Ki67 proliferation index (PI) was studied by immunohistochemistry in 22 of 25 undetected HCCs and 41 of 45 detected HCCs that had available tissue in our archives for performing immunohistochemistry. Although the PI was higher in the detected HCC group (120.8/1000 cells) compared with the undetected HCC group (81.8/1000 cells), the difference was not statistically different ($P=0.36$, Table 4). The Ki67 PI was also not significantly associated with tumor size (<2, 2 to 4, and >4 cm) (Table 4).

TABLE 4. Immunohistochemical Stainings of Ki67 Per 1000 HCC Tumor Cells and CD34 in Undetected and Detected HCCs

	Undetected HCCs (22 Tumors)	Detected HCCs (41 Tumors)	P
CD34 density (n [%])			0.002 (Fisher exact probability test)
1+ (<33%)	13 (59)	7 (17)	
2+ (33-66%)	6 (27)	28 (68)	
3+ (>66%)	3 (14)	6 (15)	
CD34 sublocation (n [%])			0.149 (Fisher exact probability test)
Central	3 (14)	3 (7)	
Peripheral	10 (45)	11 (27)	
Pan-nodular	9 (41)	27 (66)	
Ki67/1000 cells (cm)	81.8	120.8	0.36
≤1	109.1	55.7	0.45
>1-<2	30.3	155.4	0.20
2-<3	85.0	105.7	NA
3-4	136.0	171.5	0.73
>4	n/a	62.5	NA

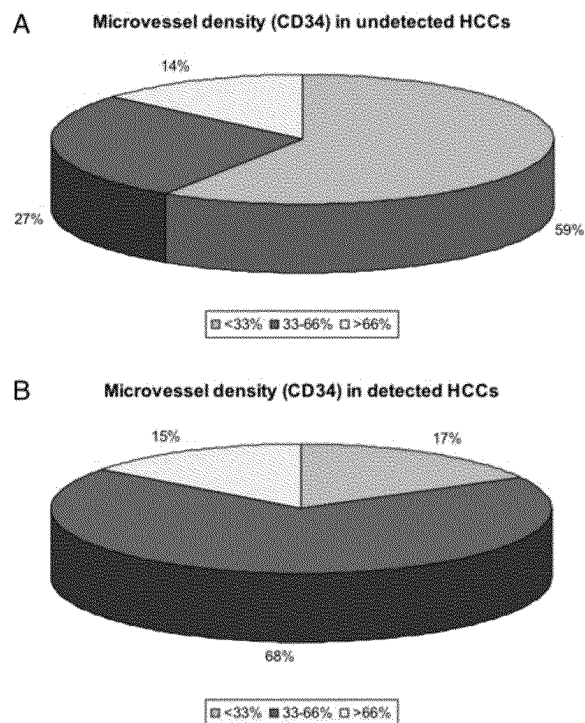
NA indicates not available.

DISCUSSION

Advances in radiology modalities has significantly improved the diagnostic accuracy for HCC in cirrhotic liver. However, undetected HCC still represents a significant portion of total HCC tumors in patients undergoing OLT. Very few studies have evaluated the pathologic features of HCCs undetected by imaging studies.^{6,7} In the current study, we have systemically analyzed the pathologic features of undetected HCCs, including tumor size, histologic differentiation, number and distribution of unpaired arteries, mitotic activity, bile production, fatty change, and Mallory-Denk bodies. We also examined sinusoidal capillarization and PI by CD34 and Ki67 immunohistochemical studies, respectively. Our data demonstrated that the undetected HCCs were small in size (<2 cm), more likely to be well differentiated, and had lower microvessel density. There were fewer unpaired arteries in the undetected HCCs compared with detected HCCs, but this difference was not statistically significant.

As expected, the size of the undetected HCCs was significantly smaller than that of the detected HCCs in our study. Within the LI-RADS algorithm, size > or <2.0 cm represents a major decision point in the scoring algorithm. The vast majority of the undetected HCCs were <2 cm. In contrast, more than half of the detected HCCs were ≥2 cm. Our findings are in complete agreement with previous reports.^{6,7} Our data again indicate that the small HCCs remain a challenge for early detection by CT-imaging studies.

We observed a significant difference in the degree of histologic differentiation between the undetected and detected HCCs. The undetected HCCs tended to be well differentiated, whereas the detected HCCs were more

**FIGURE 3.** Microvessel density by CD34 immunostaining in undetected (A) and detected (B) HCCs. The CD34 expression was significantly less diffuse in the undetected HCC group than that in the detected HCC group.

frequently moderately to poorly differentiated. The same finding was reported previously in a smaller study, but the biological explanation was not addressed.⁶ In our study, the size of the moderately to poorly differentiated HCCs in the detected group was significantly larger than that of the remaining HCCs (Fig. 2). Moreover, the moderately to poorly differentiated tumors comprised the vast majority of the detected HCCs (89%). In addition, there were more moderate to poorly differentiated tumors in the LI-RADS 4 and 5 category compared with the “not localized” and LI-RADS 3 categories ($P=0.04$) (data not shown). These observations together suggest that the size difference associated with the histologic differentiation may account for detection failure in some of the HCCs. We also examined the number of unpaired arteries, mitotic activity, as well as CD34 and Ki67 immunohistochemical profiles and although numerical differences for some of these parameters were seen between groups, only CD34 microvessel density scores achieved statistical significance. Only Ki67 PI among these features correlated well with histologic differentiation.

The liver has a dual blood supply from the portal vein and hepatic artery. The portal vein carries the majority of the blood flow (~75%), whereas the hepatic artery accounts for the remainder. HCC is one of the most vascular solid tumors, and neoangiogenesis is known to play a crucial role in all stages of tumor development.^{21,22} The neoangiogenesis of HCC is commonly characterized by an

increase of arterial blood flow and the loss of portal blood flow. Consequently, the portal blood flow decreases with the advancement of tumor, and the tumor is eventually fed predominantly by the arterial blood supply. Histologically, the distinct tumor angiogenesis in HCC is manifested by unpaired arteries, sinusoidal capillarization, and increased microvessel density, which can be demonstrated by CD34 or CD31 immunostains.²³ Importantly, hypervascularity and the altered vascular supply are also the biological ground for both the diagnosis of HCC within cirrhotic liver by 4-phase CT-imaging studies and the increased LI-RADS score given to arterial enhancing lesions and lesions with washout.^{12,13} In the arterial phase, shortly after contrast injection, HCCs manifest as hyperattenuated lesions against a background of minimally enhanced liver parenchyma in the arterial phase, because the tumor is hypervascular and predominantly supplied by the hepatic artery. Because non-neoplastic liver has a dual arterial and portal supply, the arterial phase contains lower concentration of contrast because of dilution of arterial blood by portal venous blood without contrast. In the portal/venous delayed phases, the contrast agent has been cleared from arterial blood flow and is redistributed into the portal venous blood. As a result, there is an enhancement of the surrounding non-neoplastic parenchyma but not the HCCs. This is the “washout” phenomenon seen on portal venous phase imaging. These radiologic features are considered highly specific for HCC and are the biological basis of the LI-RADS score.^{10,14,15}

Given the importance of vascular pattern for radiologic diagnosis of HCCs, we hypothesized that the number of unpaired arteries and microvessel density may contribute to the detection failure of HCCs in the pretransplant CT-imaging studies. The immunostain for CD34 has been used to evaluate microvessel density of HCCs.^{21,23,24} CD34, first identified in human hematopoietic progenitor cells, is characteristically expressed in the sinusoids of HCC but not in the adjacent non-neoplastic sinusoids.^{23,25} The CD34-positive endothelial cells in hepatocellular neoplasm are thought to represent the capillarization of sinusoids in relation to increased blood flow and pressure.²⁶ Our data showed that the undetected HCCs had significantly less CD34 immunoreactivity than the detected HCCs. The finding indicates that the low microvessel density in the undetected HCCs may contribute to the detection failure by imaging study. This notion is further supported by the findings that the enhancement features associated with HCCs at dynamic spiral CT could be correlated with tumor microvessel density.²⁷ Sinusoidal capillarization may be an aspect of hepatocarcinogenesis in which the lesions convert to the predominantly arterial blood supply associated with HCC.²⁸ It is probable that the capillarization of the sinusoids within HCCs facilitates the enhancement on arterial phase and “washout” on delayed venous phase. However, it is largely unknown as to how sinusoidal capillarization in HCC might affect CT enhancement patterns.²⁶

Unpaired arteries are defined as arteries with no accompanying bile ducts. It is known that the number of unpaired arteries is substantially lowest in cirrhotic

nodules with a gradual increase in dysplastic nodules and highest in HCC.^{26,29} The presence of the unpaired artery is a helpful histologic clue for the diagnosis of hepatocellular neoplasm. In our study, the number of unpaired arteries was slightly fewer in the undetected HCCs than in the detected HCCs (Table 2). However, the difference was not statistically significant. The unpaired arteries were also not significantly different when we controlled for the CD34 distribution or histologic differentiation. Our data thus suggest that the number of unpaired arteries within HCCs may not account for the detection failure by CT imaging. In a previous study, the degree of contrast enhancement in the arterial phase tended to correlate with the number of unpaired arteries in CT-detected HCCs.²⁶ A different study, however, suggested that the number of unpaired arteries had only a weak correlation with the attenuation level on CT imaging.³⁰ In addition to the arterial blood flow, it is probable that the microvascular permeability, blood volume, and the extent of extracellular space may also play an important role in the contrast enhancement of a lesion.^{26,30} Further studies are needed to examine how the number of unpaired arteries influence the radiologic features in HCCs by CT-imaging studies.

Chronic hepatitis is characterized by increased regenerative cell proliferation that makes cells more susceptible to gene mutations. The Ki67 PI was found to be substantially increased in cirrhotic liver as transition from the nondysplastic nodule, to dysplastic nodules, and finally to HCC occurs.^{27,31} However, the relationship between Ki67 PI and radiologic detection of HCCs has not previously been examined. To our knowledge, our study is the first one to evaluate Ki67 PI in this context. Our data did not identify a statistically significant association between Ki67 PI and detection failure by CT imaging in HCCs. This may be because of the small number of cases in the study. Alternatively, imaging modalities based on the extent of vascular enhancement may not distinguish differences in proliferation of the HCC tumor cells.

There were several limitations in our study. First, the study was retrospective and had a small sample size. Second, CT report was used as the criteria for undetected versus detected HCCs. Systematic retrospective review session of CT images was not performed. In addition, CTs performed >90 days but no more than 180 days before transplantation were included in the evaluation to increase the case number. HCC grows over time; hence, increasing the time window in which cases were included is a limitation to the study, because in selected cases, final pathologic features may not be fully represented by available imaging data.

In summary, our data indicate that the contributing factors for detection failure in HCCs by the pretransplant CT-imaging studies include small tumor size (<2 cm), low-grade histologic differentiation, and low microvessel density. These observations emphasize the evolving importance of LI-RADS assessment in liver transplant candidates. Notably, a significant association between the number of unpaired arteries and HCC detection has not been established by our study.

REFERENCES

1. Kudo M. Management of hepatocellular carcinoma: from prevention to molecular targeted therapy. Proceedings of the 3rd International Kobe Liver Symposium on HCC with an International Liver Cancer Association (ILCA) Scientific Session. Hyogo, Japan, June 6-7, 2009. *Oncology*. 2010;78(suppl 1):1-190.
2. El-Serag HB. Hepatocellular carcinoma: recent trends in the United States. *Gastroenterology*. 2004;127:S27-S34.
3. Llovet JM, Bruix J. Novel advancements in the management of hepatocellular carcinoma in 2008. *J Hepatol*. 2008;48(suppl 1):S20-S37.
4. Bruix J, Sherman M. Practice Guidelines Committee American Association for the Study of Liver Diseases. Management of hepatocellular carcinoma. *Hepatology*. 2005;42:1208-1236.
5. Mazzaferro V, Chun YS, Poon RT, et al. Liver transplantation for hepatocellular carcinoma. *Ann Surg Oncol*. 2008;15:1001-1007.
6. Urahashi T, Lynch SV, Kim YH, et al. Undetected hepatocellular carcinoma in patients undergoing liver transplantation: is associated with favorable outcome. *Hepatogastroenterology*. 2007;54:1192-1195.
7. Achkar JP, Araya V, Baron RL, et al. Undetected hepatocellular carcinoma: clinical features and outcome after liver transplantation. *Liver Transpl Surg*. 1998;4:477-482.
8. Lee J, Lee WJ, Lim HK, et al. Early hepatocellular carcinoma: three-phase helical CT features of 16 patients. *Korean J Radiol*. 2008;9:325-332.
9. Lencioni R, Piscaglia F, Bolondi L. Contrast-enhanced ultrasound in the diagnosis of hepatocellular carcinoma. *J Hepatol*. 2008;48:848-857.
10. Lee KH, O'Malley ME, Haider MA, et al. Triple-phase MDCT of hepatocellular carcinoma. *Am J Roentgenol*. 2004;182:643-649.
11. Sakamoto M, Hirohashi S, Shimozato Y. Early stages of multistep hepatocarcinogenesis: adenomatous hyperplasia and early hepatocellular carcinoma. *Hum Pathol*. 1991;22:172-178.
12. Forner A, Rodríguez De Lope C, Reig M, et al. Treatment of advanced hepatocellular carcinoma. *Gastroenterol Hepatol*. 2010;33:461-468.
13. Fernández M, Semela D, Bruix J, et al. Angiogenesis in liver disease. *J Hepatol*. 2009;50:604-620.
14. Matsui O. Imaging of multistep human hepatocarcinogenesis by CT during intra-arterial contrast injection. *Intervirology*. 2004;47:271-276.
15. Bolondi L, Gaiani S, Celli N, et al. Characterization of small nodules in cirrhosis by assessment of vascularity: the problem of hypovascular hepatocellular carcinoma. *Hepatology*. 2005;42:27-34.
16. American College of Radiology Liver Imaging Reporting and Data System, version 2014. 2014. Available at: www.acr.org/Quality-Safety/Resources/LIRADS.
17. Mita K, Kim SR, Kudo M, et al. Diagnostic sensitivity of imaging modalities for hepatocellular carcinoma smaller than 2 cm. *World J Gastroenterol*. 2010;16:4187-4192.
18. Nakashima Y, Nakashima O, Hsia CC, et al. Vascularization of small hepatocellular carcinomas: correlation with differentiation. *Liver*. 1999;19:12-18.
19. Kudo M, Izumi N, Kokudo N, et al. Management of hepatocellular carcinoma in Japan: Consensus-Based Clinical Practice Guidelines proposed by the Japan Society of Hepatology (JSH) 2010 updated version. *Dig Dis*. 2011;29:339-364.
20. Bosman F, CF, Hruban, RH, Theise, ND. *WHO Classification of Tumours of the Digestive System*. Lyon: IARC Press; 2010.
21. Park JO, Yeh MM. Clinical significance and implication of neoangiogenesis in hepatocellular carcinoma. *J Gastroenterol Hepatol*. 2011;26:792-793.
22. Hayashi M, Matsui O, Ueda K, et al. Correlation between the blood supply and grade of malignancy of hepatocellular nodules associated with liver cirrhosis: evaluation by CT during intraarterial injection of contrast medium. *Am J Roentgenol*. 1999;172:969-976.
23. Kimura H, Nakajima T, Kagawa K, et al. Angiogenesis in hepatocellular carcinoma as evaluated by CD34 immunohistochemistry. *Liver*. 1998;18:14-19.
24. Asayama S, Sekine T, Kawakami H, et al. Synthesis of aminated poly(1-vinylimidazole) for a new pH-sensitive DNA carrier. *Nucleic Acids Symp Ser (Oxf)*. 2007:333-334.
25. Poon RT, Fan ST, O'Suilleabhain CB, et al. Aggressive management of patients with extrahepatic and intrahepatic recurrences of hepatocellular carcinoma by combined resection and locoregional therapy. *J Am Coll Surg*. 2002;195:311-318.
26. Kim CK, Lim JH, Park CK, et al. Neoangiogenesis and sinusoidal capillarization in hepatocellular carcinoma: correlation between dynamic CT and density of tumor microvessels. *Radiology*. 2005;237:529-534.
27. Chen WX, Min PQ, Song B, et al. Single-level dynamic spiral CT of hepatocellular carcinoma: correlation between imaging features and density of tumor microvessels. *World J Gastroenterol*. 2004;10:67-72.
28. Haratake J, Hisaoka M, Yamamoto O, et al. An ultrastructural comparison of sinusoids in hepatocellular carcinoma, adenomatous hyperplasia, and fetal liver. *Arch Pathol Lab Med*. 1992;116:67-70.
29. Park YN, Kim YB, Yang KM, et al. Increased expression of vascular endothelial growth factor and angiogenesis in the early stage of multistep hepatocarcinogenesis. *Arch Pathol Lab Med*. 2000;124:1061-1065.
30. Asayama Y, Yoshimitsu K, Irie H, et al. Poorly versus moderately differentiated hepatocellular carcinoma: vascularity assessment by computed tomographic hepatic angiography in correlation with histologically counted number of unpaired arteries. *J Comput Assist Tomogr*. 2007;31:188-192.
31. Yeh MM, Larson AM, Campbell JS, et al. The expression of transforming growth factor- α in cirrhosis, dysplastic nodules, and hepatocellular carcinoma: an immunohistochemical study of 70 cases. *Am J Surg Pathol*. 2007;31:681-689.